

Time-frequency analysis based on curvelet transforms with time skewing

Jiao Wang^{1*}, Zhenchun Li¹, Lutz Gross² and Stephen Tyson³

¹School of Geosciences, China University of Petroleum, Qingdao, 266580, China, ²School of Earth and Environmental Sciences, the University of Queensland, Brisbane, Australia, and ³School of Petroleum Engineering, Universiti Teknologi Brunei, Gadong, Brunei Darussalam

Received December 2018, revision accepted April 2019

ABSTRACT

Oil and gas exploration gradually changes to the deep and complex areas. The quality of seismic data restricts the effective application of conventional time-frequency analysis technology, especially in the case of low signal-to-noise ratio. To address this problem, we propose a curvelet-based time-frequency analysis method, which is suitable for seismic data, and takes into account the lateral variation of seismic data. We first construct a kind of curvelet adapted to seismic data. By adjusting the rotation mode of the curvelet in the form of time skewing, the scale parameter can be directly related to the frequency of the seismic data. Therefore, the curvelet coefficients at different scales can reflect the time-frequency information of the seismic data. Then, the curvelet coefficients, which represent the dominant azimuthal pattern, are converted to the time-frequency domain. Since the curvelet transform is a kind of sparse representation for the signal, the screening process of the dominant coefficient masks most of the random noise, which enables the method to adapt for the low signal-to-noise ratio data. Results of synthetic and field data experiments using the proposed method demonstrate that it is a good approach to identify weak signals from strong noise in the time-frequency domain.

Key words: Curvelet, Noise, Time-frequency, Time skewing .

INTRODUCTION

In signal processing, commonly used time-frequency analysis methods include: short-time Fourier transform, Gabor transform, wavelet transform, Wigner transform, fractional Fourier transform, Hilbert–Huang transform and synchrosqueezing transform. These methods are able to resolve the relationship between frequency and time, but when the signal-to-noise ratio (SNR) is low, the effective weak signal is submerged in the noise, and traditional time-frequency analysis methods cannot identify useful information.

Wavelet transform is a widely used multi-scale transform. It has a good ability to capture the local singularity of non-stationary signals (Mallat 1989). This ability can

be exploited in the case of one-dimensional signal whose singularity generally appears to be point singular. However, linear singularity and curve singularity are more important for two-dimensional signals, which means that wavelets have strong limitations when applied in more than one dimension. Candès (1998) developed ridgelets: a new method which can effectively deal with linear singularities in two-dimensional signals. On this basis, Candès and Donoho (1999, 2004) proposed the curvelet transform. It can efficiently present the images with curve edge, dealing with higher singularities compared to wavelet and ridgelet transforms. Curvelet transform are widely used in seismic exploration due to its favourable properties, such as multi-scale analysis and multi-directional analysis. Its main applications are to separate signal and noise, including random noise removal (Neelamani *et al.* 2008; Kustowski *et al.* 2013; Górszczyk, Malinowski and Bellefleur

*E-mail: wangjiao0918@gmail.com

2015; Dong *et al.* 2017), surface wave suppression (Yarham, Boeniger and Herrmann 2006; Boustani *et al.* 2013), multiple attenuation (Herrmann, Böniger and Verschuur 2007; Donno, Chauris and Noble 2010); seismic data interpolation and recovery (Herrmann and Hennenfent 2008; Naghizadeh and Sacchi 2010; Shahidi *et al.* 2013); sparse deconvolution (Kumar and Herrmann 2008); amplitude versus offset inversion (Hennenfent and Herrmann 2004); migration imaging (Douma and de Hoop 2004; Chauris and Nguyen 2008). Their results show that the curvelet transform has a great advantage on the analysis and processing of seismic data.

Curvelet transform can be used to sparsely represent an image, and differentiate between continuous signal and random noise in terms of the curvelet coefficient values. Comparing with the wavelet transform, the curvelet transform is less sensitive to noise. Moreover, the effective information in the curvelet domain is moderate redundancy, and contains the energy distributions at different scales, angles and locations. This information may reflect some special properties of the formation, especially for anisotropy. Conventional curvelet transforms use rotations in the image space to align wavelet with image features. When applied to seismic track in the time-space domain, this approach would lead to energy leakage between traces, which reduces the frequency resolution. To avoid this issue, we replace the rotation by skewing in time direction. In this way, the curvelet coefficient can reflect the time-frequency information of the seismic data.

In addition, the traditional time-frequency analysis is suitable for one-dimensional signal, and ignores their lateral variation. For data with low SNR, the effective information cannot be accurately identified. Although the two-dimensional time-frequency analysis method has been developed (Mansinha, Stockwell and Lowe 1997), the time-frequency data produced using this method has large redundancy, low computational efficiency and high memory cost. This limits its widely application. The method proposed in this paper can not only avoid these problems, but also produce good time-frequency results.

The key idea of the method is to establish relationship between curvelet coefficients and time-frequency, which can improve the effectiveness of time-frequency analysis for seismic data in complex areas with low SNR. First, we will briefly review the basic properties of the wavelet transform, the ridgelet transform and the continuous curvelet transform, respectively. We will then construct a kind of curvelet adapted to seismic data, replace the traditional rotation mode of the curvelet by time skewing; thus, pick the curvelet coefficients at the optimal angle and convert them to the time-frequency domain. In order to improve the time-frequency resolution, we will

apply the synchrosqueezing transform into the curvelet-based time-frequency analysis method in this paper. Finally, inclination models and field data with different SNR will be tested. Results are compared with wavelet transform to demonstrate the ability of our modified curvelet transform.

THEORY

Wavelet transform and ridgelet transform

The continuous wavelet transform (CWT) of a signal $s(t) \in L^2(\mathbb{R})$ is defined as

$$\text{CWT}(b, a) = \int s(t) \frac{1}{\sqrt{a}} \varphi^* \left(\frac{t-b}{a} \right) dt, \quad (1)$$

where φ is the ‘mother’ wavelet, φ^* is the complex conjugate of φ , a and b are the scale and translation factors, respectively. The mother wavelet can provide a source function to generate a series of wavelets which are simply the scaled and translated versions of the mother wavelet. Wavelet transform can effectively present the point singularities for one-dimensional signals, while ridgelet transform exhibits high directional sensitivity, and this feature makes it suitable for two-dimensional signals.

Given a two-dimensional time-space domain signal $s(t, x) \in L^2(\mathbb{R}^2)$, its continuous ridgelet transform (CRT) can be defined as

$$\text{CRT}(a, b, \theta) = \iint_{t,x} s(t, x) \varphi_{a,b,\theta}^*(t, x) dt dx, \quad (2)$$

where ridgelets $\varphi_{a,b,\theta}(t, x)$ in two-dimensional are defined from a wavelet-type function in one-dimensional as

$$\varphi_{a,b,\theta}(t, x) = \frac{1}{\sqrt{a}} \varphi \left(\frac{t \cos \theta + x \sin \theta - b}{a} \right), \quad (3)$$

where θ is the rotation factor. Figure 1 shows a ridgelet and its scaled, shifted and rotated versions. Ridgelets are constant along ridgelet lines $t \cdot \cos \theta + x \cdot \sin \theta$ and are equal to the wavelets in the orthogonal direction.

Continuous curvelet transform

For signal $s(t, x)$, its continuous curvelet transform is a sparse representation of the inner product of basis functions with the signal, which is defined as

$$\begin{aligned} \text{CT}(a, \theta, k) &= \langle s(t, x), \varphi_{a,\theta,k}(t, x) \rangle \\ &= \iint_{t,x} s(t, x) \varphi_{a,\theta,k}^*(t, x) dt dx. \end{aligned} \quad (4)$$

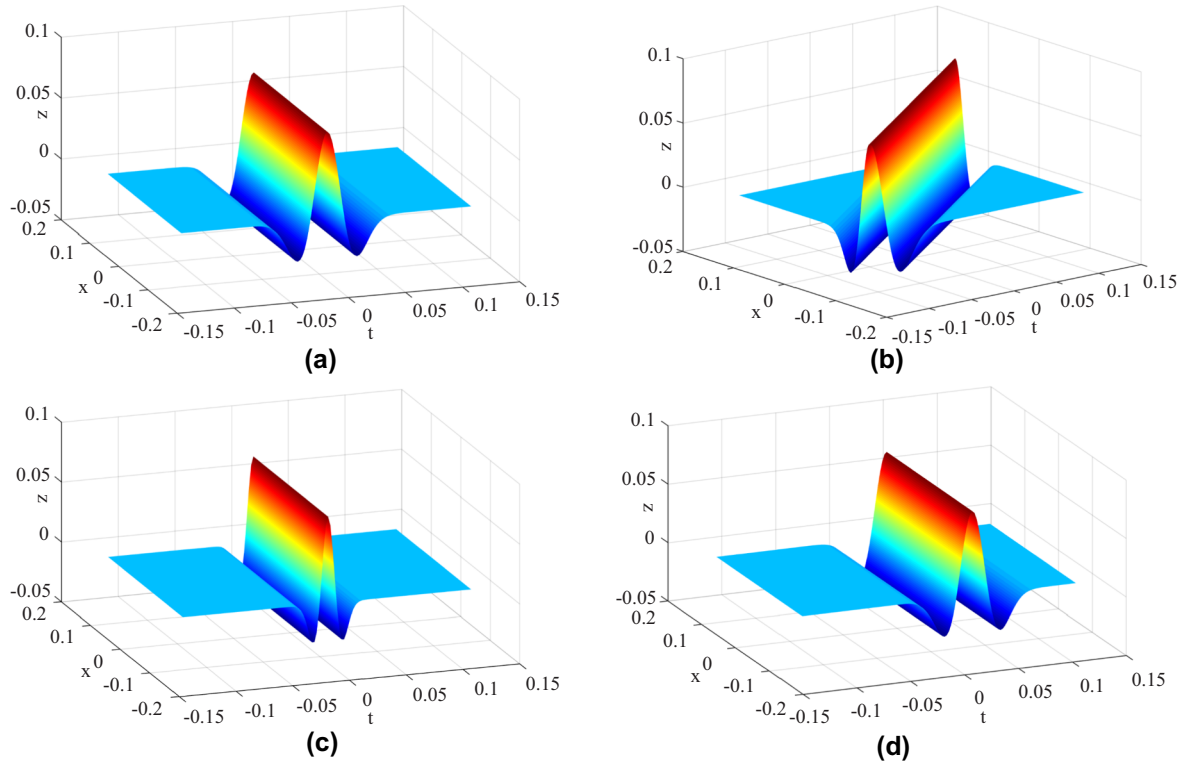


Figure 1 Few Ridgelets examples. (a) A ridgelet function. From (b) to (d) are rotated, scaled and translated versions of (a), respectively.

The curvelet coefficient is the projection of $s(t, x)$ onto the curvelet function $\varphi_{a,\theta,k}^*(t, x)$, parameterized by a , k , and θ . The multi-scale property and anisotropy of the curvelet transform are determined by the basis function

$$\varphi_{a,\theta,k}^*(t, x) = a^{-\frac{3}{4}} \varphi \left[R_\theta \left(\frac{t - \tau}{a}, \frac{x - \varepsilon}{\sqrt{a}} \right) \right], \quad (5)$$

where φ is ‘mother’ curvelet, $k = [\tau, \varepsilon]$ is the translation vector in the two-dimensional space-time plane and θ is the azimuth parameter. The function $R_\theta(t, x)$ represents the rotation of the vector (t, x) by angle θ , which is given by

$$R_\theta(t, x) = (t \cos \theta + x \sin \theta, x \cos \theta - t \sin \theta). \quad (6)$$

That is to say, we can get the curvelet function $\varphi_{a,\theta,k}^*(t, x)$ from the mother curvelet φ through translation in the direction of vector $k = [\tau, \varepsilon]$ and subsequent scale stretching and azimuth rotation.

An image can be represented by a series of curvelets. The anisotropy appears as that for the image $s(t, x)$ with a linear edge, corresponding curvelet coefficient differs when the direction is different, even though they have the same scale and position. As shown in Fig. 2, at the edge of the curve highlighted in blue, the position and scale of curvelet A and curvelet B are both the same, but their orientation angles are

different. We can see that the coefficient $CT(a, \theta, k)$ of curvelet A, whose trend is aligned with the curve, is much larger than that one of curvelet B. For an isotropic point feature, as shown in right bottom corner of Fig. 2, the corresponding coefficients of curvelets with orientation in any direction but with the same scale and position are approximately equal. In terms of energy distribution, the main energy of the linear feature is focused at individual curvelet coefficients in that position and aligned orientation, while the energy of point-like features is divided to all curvelets in the corresponding position. This result of an improved separation of features in an image from random noise, which defines a point-like feature.

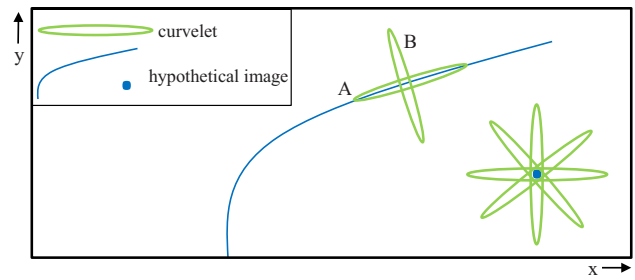


Figure 2 Anisotropy in curvelet transform.

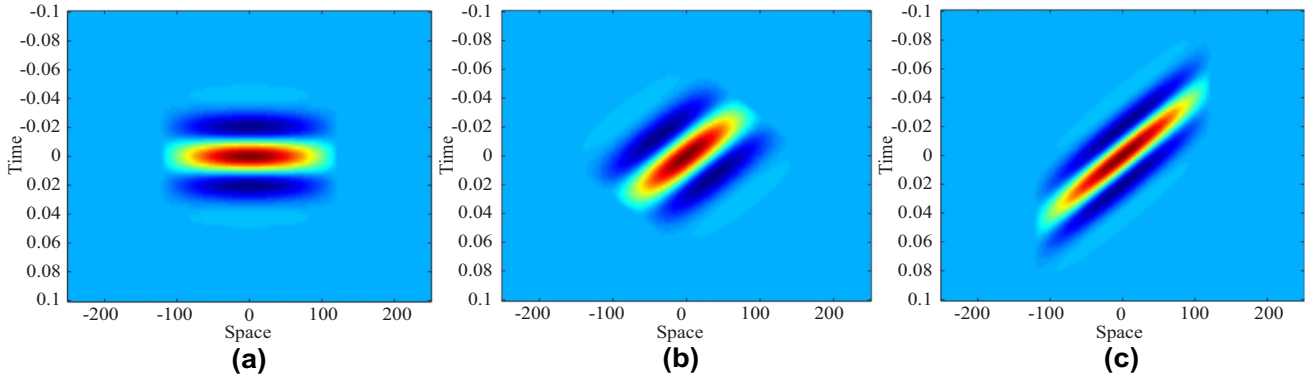


Figure 3 (a) Curvelet before rotation. (b) Traditional curvelet rotation by $\frac{\pi}{4}$. (c) Proposed curvelet pseudo-rotation by $\frac{\pi}{4}$.

A specialized curvelet transform

In the studies of Candès and Donoho (2004), the mother curvelet $\varphi(t, x)$ is obtained by binary division of angle and scale in two-dimensional Fourier domain, which assumes that the signal $s(t, x)$ has the similar physical characteristics and scale in different dimensions. To some extent, this assumption limits the scope of the curvelet transform in seismic analysis, because the seismic data use different physical quantities in the time direction t and space direction x .

In order to make the mother curvelet adapt to the seismic wave characteristics, and to ensure the relative independence

in time and space dimension, we construct the mother curvelet in the space-time domain. The time domain is based on Morlet wavelet, while the space domain uses the limited range of Hanning window:

$$\varphi(t, x) = \begin{cases} \pi^{-1/4} e^{i2\pi f_0 t} e^{-t^2/2} \cos(\pi x/2\lambda), & |x| \leq \lambda \\ 0, & |x| > \lambda \end{cases}, \quad (7)$$

where f_0 is the dominant frequency of the mother curvelet and λ is the extension range of the mother curvelet in the spatial domain. Its value is proportional to the wavelength, and we choose twice the wavelength in this paper, that is, $\lambda = \frac{2v_0}{f_0}$, where, v_0 is the background seismic velocity. When

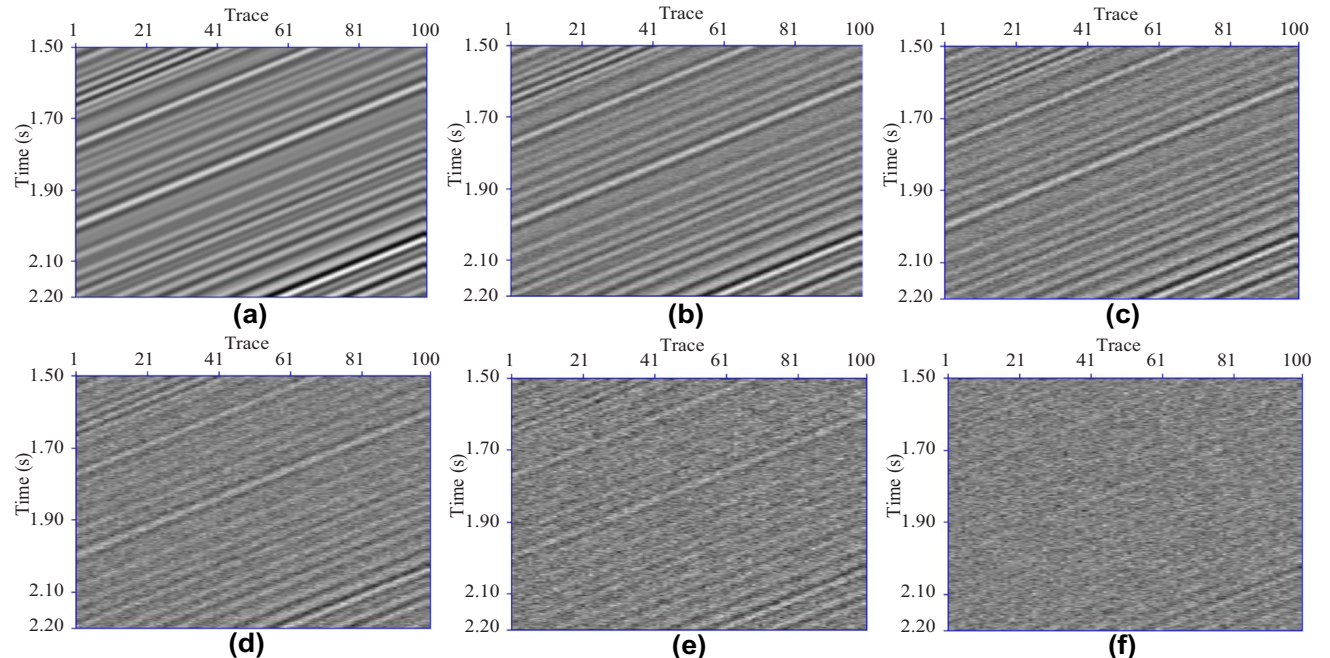


Figure 4 Simulated models with different SNR. (a) Noise-free. (b) SNR = 20 db. (c) SNR = 10 db. (d) SNR = 0 db. (e) SNR = -10 db. (f) SNR = -20 db.

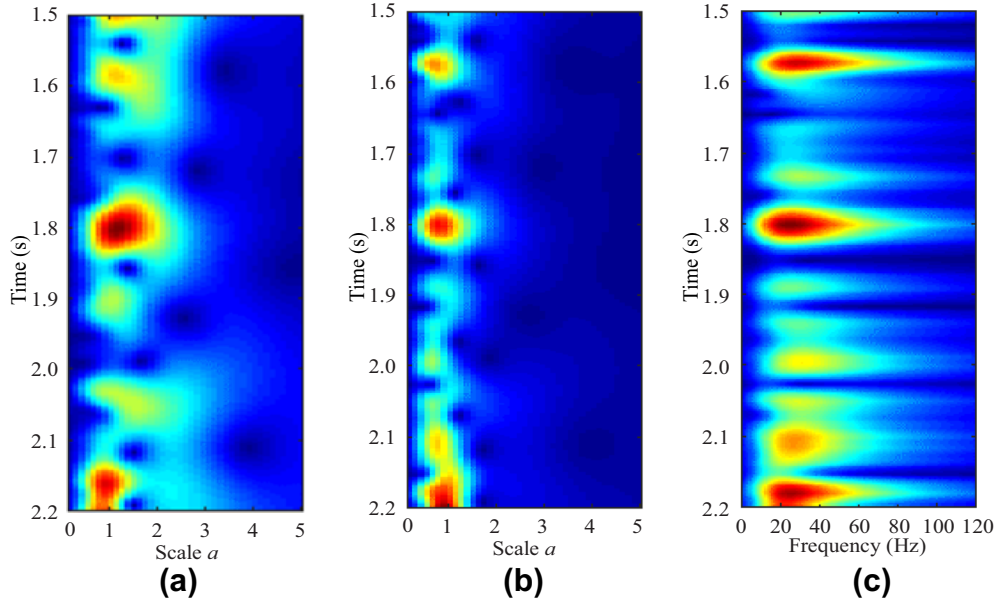


Figure 5 Curvelet coefficients and its time-frequency analysis of 50th trace in Fig. 4(a). (a) Curvelet coefficient when SCT's angle is 0. (b) OASCT coefficients. (c) Time-frequency map by the method proposed.

λ is infinite, there is no scale change in the horizontal, which is equivalent to the ridgelet. When λ is close to 0, there is no lateral extension, which is equivalent to the one-dimensional wavelet function.

In general, the angle of rotation of the curvelet is computed by equation (6). It is easy to obtain the relationship

between the dominant frequency f_c and the scale parameter α and angle θ in the time direction of the curvelet.

$$f_c(\alpha, \theta) = f_0 / \left(\frac{\alpha}{\cos \theta} \right). \quad (8)$$

Because the longitudinal and lateral information of seismic data are in the time and spatial domain respectively,

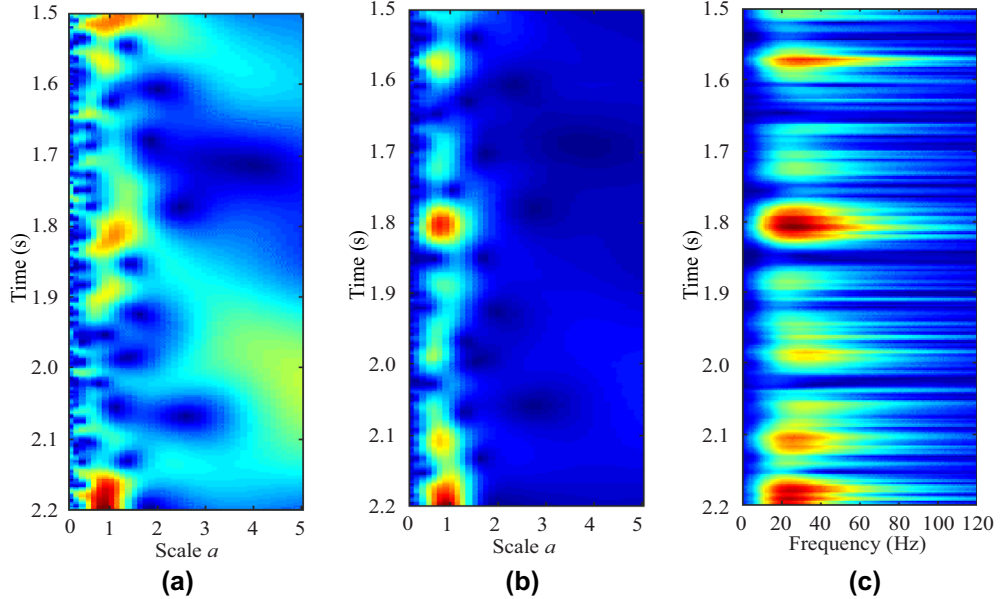


Figure 6 Curvelet coefficients and its time-frequency analysis of 50th trace in Fig. 4(d). (a) Curvelet coefficient when SCT's angle is 0. (b) OASCT coefficients. (c) Time-frequency map by the method proposed.

parameter θ in this equation is mixed with different domain information, and the frequency is difficult to estimate. Therefore, we replace the rotation function $R_\theta(t, x)$ by the time skewing transformation,

$$R'_\theta(t, x) = \left(t + \operatorname{sgn}(t) \frac{x}{v_0} \tan\theta, x \right), \quad \theta \in \left(-\frac{\pi}{2}, \frac{\pi}{2} \right). \quad (9)$$

In this case, θ is considered to be an estimate of the ground inclination targeted by the curvelet transform, and thus it has some geophysical significance.

Figure 3(a) is a sketch of a curvelet before any rotation in space-time domain. Figure 3(b,c) shows the rotated curvelet with the traditional rotation and the time-shifted, pseudo-rotation, respectively. In Fig. 3(c), the proposed time skewing applies a time shift only, but it does not affect the frequency of the curvelet in time direction, so that the frequency of the curvelet can be corresponding to the scale a . This is conducive for any time-frequency analysis.

It is worth mentioning that ridgelets are constant along ridgelet lines, and as the scale a changes, only the orthogonal direction of the ridgelets changes, while the support range along the ridgelet lines remains the same (Fig. 1c). In contrast, the values along the ridge of the mother curvelet constructed in this paper are variable, and as the scale changes, the expansion and contraction arises both in the time direction and the spatial direction. That is, the basis function of the method is a narrow two-dimensional basis function with variable scale and variable azimuth. It has the characteristics of the curvelet and is more advantageous than the ridgelet transformation.

In this case, the expression of the curvelet transform can be written as

$$\begin{aligned} \text{SCT}(a, \theta, t, x) = a^{-3/4} \iint s(t - \tau, x - \varepsilon) \\ \varphi^* \left(\frac{-\tau - \operatorname{sgn}(\tau) \frac{\varepsilon}{v_0} \cdot \tan\theta}{a}, \frac{-\varepsilon}{\sqrt{a}} \right) d\tau d\varepsilon. \end{aligned} \quad (10)$$

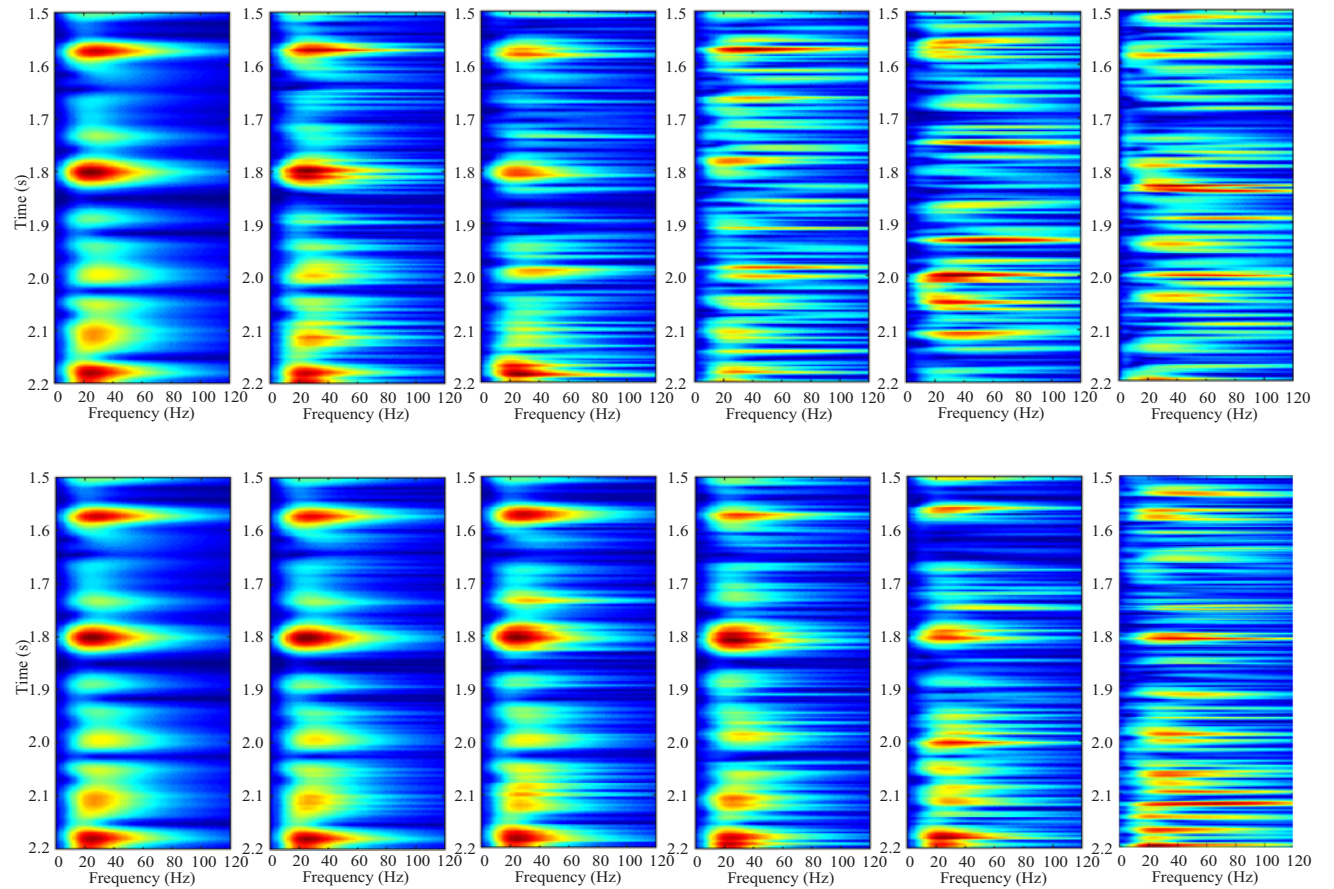


Figure 7 Time-frequency analysis of 50th trace in Fig. 4 with different SNR. Top row: CWT, bottom row: specialized curvelet transform. SNR from left to right: noise-free, 20 db, 10 db, 0 db, -10 db, -20 db.

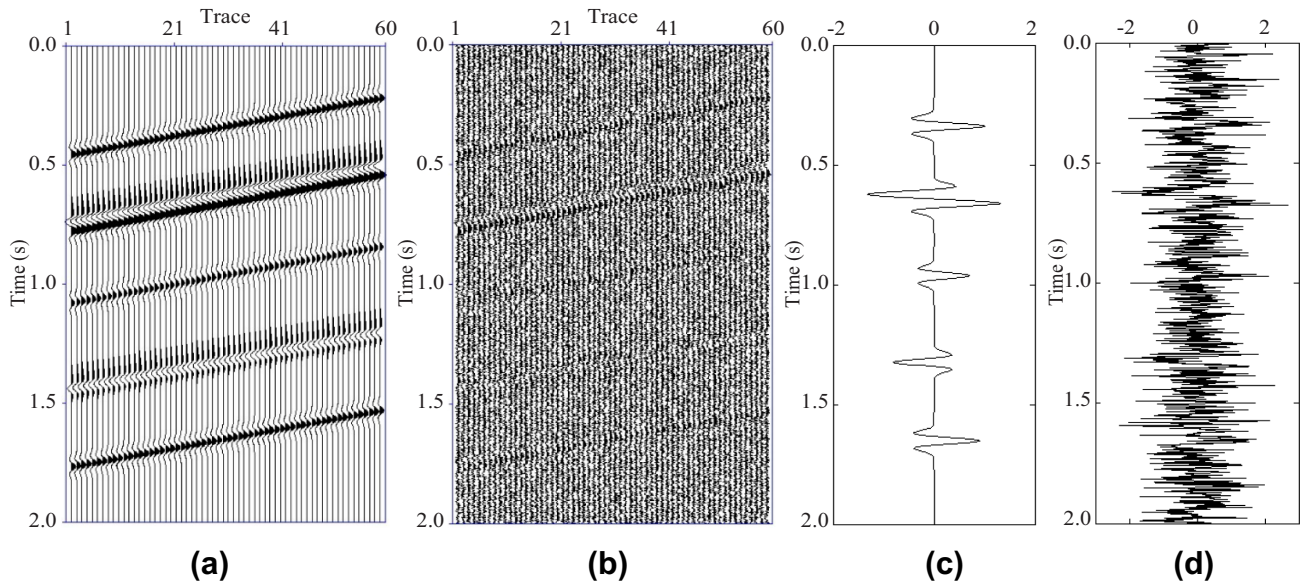


Figure 8 (a) Model. (b) Model with random noise added. (c) Single-trace signal corresponding to model (a). (d) Single-trace signal corresponding to model (b). Horizontal axis is CDP offset and vertical axis is time.

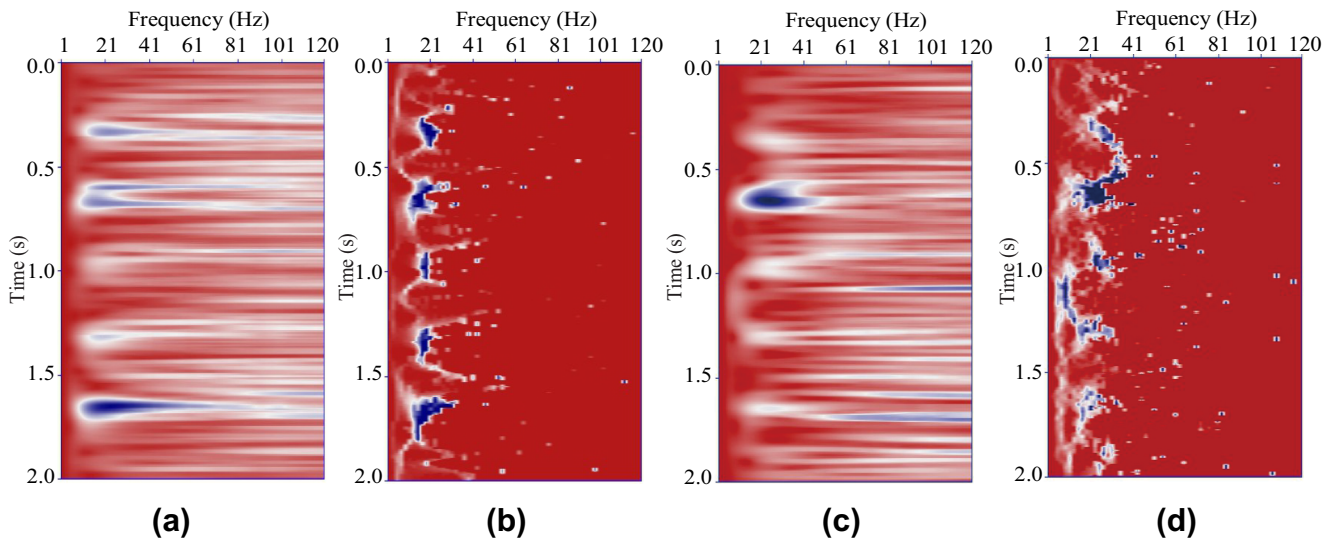


Figure 9 (a) Specialized curvelet transform. (b) Synchrosqueezing specialized curvelet transform. (c) Conventional wavelet transform. (d) Synchrosqueezing wavelet transform. Red and blue define areas with low and high energy, respectively.

This equation can be understood as a specialized equation of the curvelet transform, which is more suitable to apply in the analysis of seismic data. Here, we have defined it as the Specialized Curvelet Transform.

Since in this transform, θ does not weight the scale parameter a of the t and x components, a becomes the only variable that needs discussion in the multi-scale analysis. So, a is directly related to the frequency information. Moreover, we

carry out the analysis on continuous scale and angle, which effectively improve time-frequency analysis abilities on seismic data.

Time-frequency analysis by curvelet transform

In equation (10), the curvelet coefficient $SCT(a, \theta, t, x)$ contains parameters in four dimensions, where θ has strong focusing ability towards azimuth information in the signal.

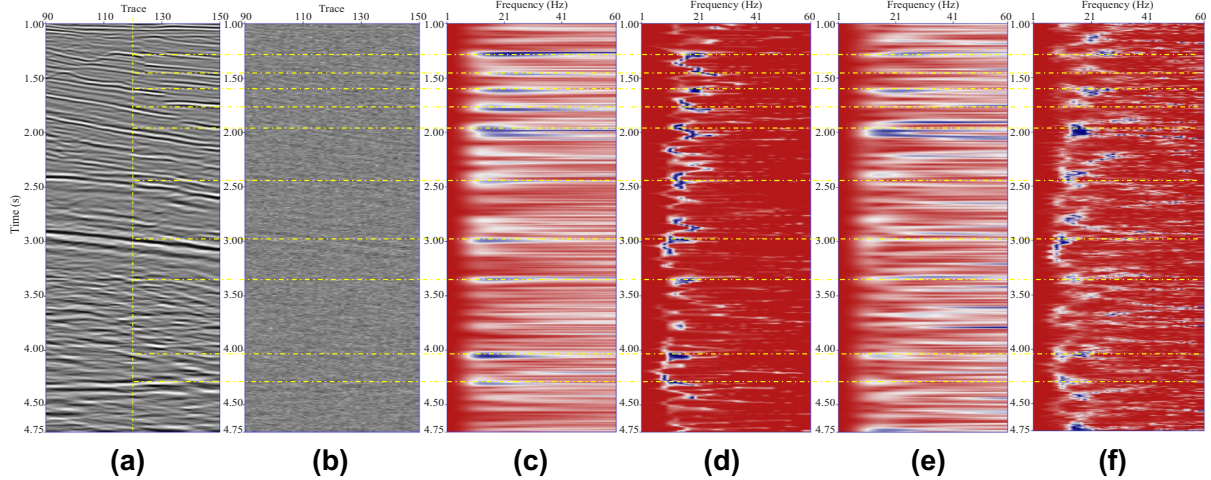


Figure 10 (a) Original profile. (b) Profile with noise. Different time-frequency analysis of 120th trace in profile (b). (c) Specialized curvelet transform. (d) Synchrosqueezing specialized curvelet transform. (e) Wavelet transform. (f) Synchrosqueezing wavelet transform.

So, we can perform optimization to solve θ and carry out multi-scale analysis on a certain seismic trace $x = x_i$,

$$\hat{\theta}_t := \left| \int \text{SCT}_{x_i}(a, \theta, t) da \right| \rightarrow \max, \quad \text{over } \theta \in \left(-\frac{\pi}{2}, \frac{\pi}{2} \right), \quad (11)$$

where $\hat{\theta}_t$ is the optimum angle corresponding to the maximum value of the curvelet coefficient at time t . It is the inclination under which the curvelets match the reflection event best. The curvelet coefficient at this inclination is least sensitive to noise. And then the corresponding curvelet coefficient of the seismic trace can be expressed as

$$\text{OASCT}_{x_i}(a, t) = \text{SCT}_{x_i}(a, \hat{\theta}_t, t). \quad (12)$$

OASCT represents the special curvelet transform with optimized angle. As the curvelet coefficient value $\text{OASCT}_{x_i}(a, t)$ depends on the scale and time parameters only, we can use it as a mean for time-frequency analysis. The angle θ and scale a are independent of each other in time direction in equation (10), which makes it possible for curvelet transform applied in time-frequency analysis of seismic data. We can employ the conversion equation for the wavelet coefficients to time-frequency domain. Here, we use the time-frequency continuous wavelet transform approach proposed by Sinha *et al.* (2005) for reference

$$F_{x_i}(f, t) = \int_{-\infty}^{+\infty} \text{OASCT}_{x_i}(a, t) \hat{\phi}(af) e^{-i2\pi ft} \frac{da}{a^{3/2}}, \quad (13)$$

where $\hat{\phi}(af)$ is the Fourier transform of $\phi(t, 0)$ in equation (7), which is the Morlet wavelet in frequency domain with dominant frequency f_0 . $F_{x_i}(f, t)$ is the time-frequency analysis cor-

responding to the optimal curvelet coefficient obtained by performing the specialized curvelet transform on the x_i th spatial channel of the seismic data.

NUMERICAL EXAMPLES

Synthetic experiments

In order to verify the adaptability of the proposed method to different noisy signals, a set of model data is tested (Fig. 4a). Taking the actual seismic as reference, the synthetic seismic record of the i th ($i = 1, 2, \dots, 100$) channel is obtained by convolving the reflection coefficients and time-varying seismic wavelet

$$s_i(t) = \sum r_i(t + \tau) w_{f(t-\tau)}(\tau), \quad (14)$$

where $r_i(t) = r_{i-1}(t - dt)$, $r_i(t)$ is a series of random reflection coefficients, dt is the time sampling interval and the seismic wavelet selects the Morlet wavelet as the following expression

$$w_f(t) = e^{-t^2} e^{i2\pi ft}. \quad (15)$$

In this model, the dominant frequency of the wavelet is linearly attenuated with time $f(t) = 40 - 5t$ Hz. The time t varies from 1.5 s to 2.2 s, thus the dominant frequency is gradually reduced from 32.5 to 29 Hz. White noise is gradually added to the simulated data. The signal-to-noise ratios (SNRs) of the images after adding noise are 20 db, 10 db, 0 db, -10db and -20 db, respectively. The signal-to-noise ratio is expressed as $\text{SNR} = 20\log_{10} \frac{\|s\|}{\|n\|}$.

Figure 5 shows the results of time-frequency analysis of the 50th trace of the model without noise. Figure 5(a) is

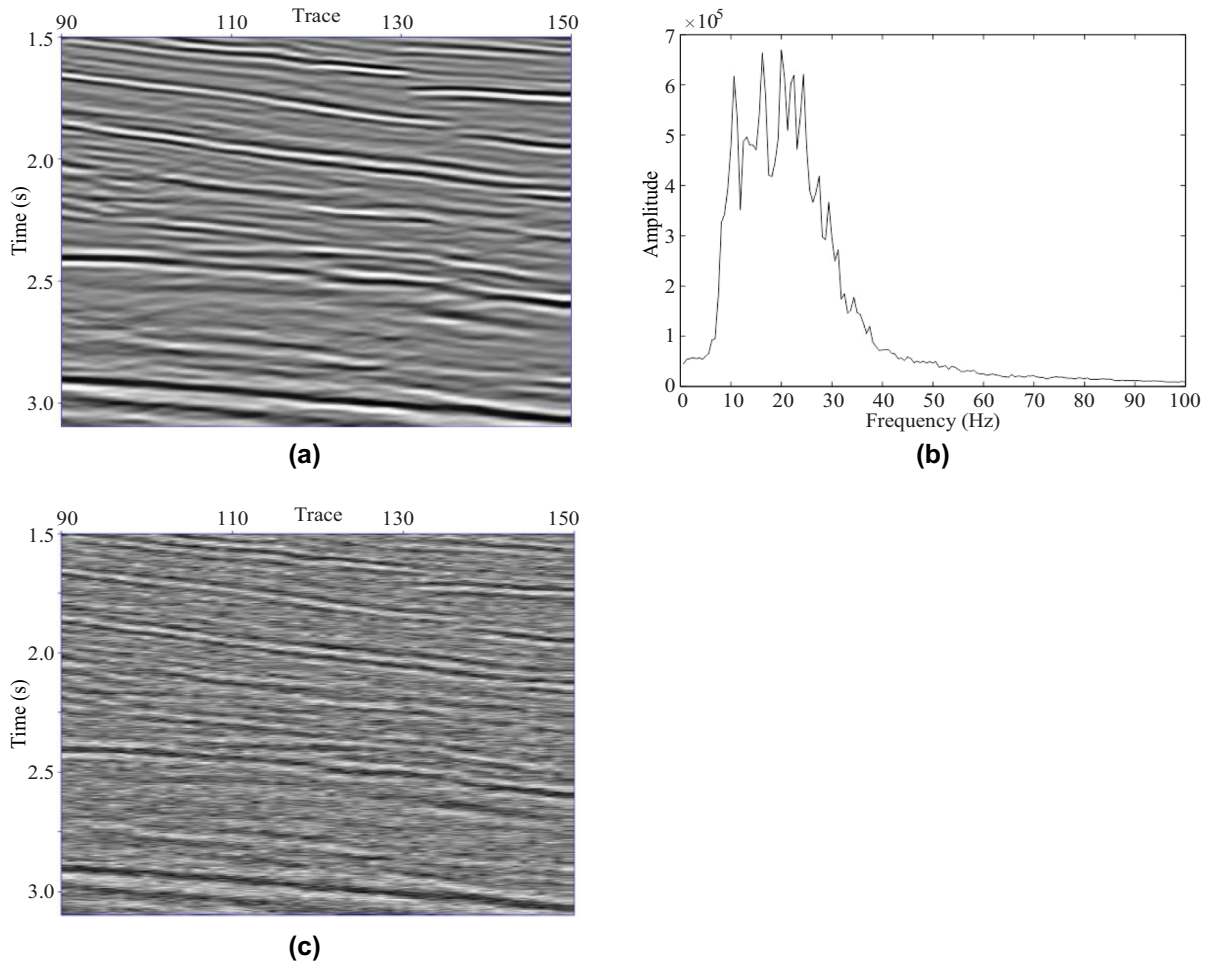


Figure 11 (a) Partial original, multi-trace profile. (b) Amplitude spectrum of the original profile. (c) Profile with added noise (SNR = -4.05 db).

the curvelet coefficients $SCT_{x_{50}}(a, 0, t)$ when the angle $\theta = 0$, Fig. 5(b) is the angle-optimized curvelet coefficients $OASCT_{x_{50}}(a, t)$ and Fig. 5(c) is the time-frequency map $F_{x_{50}}(f, t)$ after the optimal curvelet coefficient conversion. Figure 6 shows the curvelet coefficients and their corresponding time-frequency map of the 50th trace of the noisy model at SNR = 0. For the inclined layer, the optimized curvelet coefficient is more concentrated than the zero-angle curvelet coefficients, because the former can locate the position of the effective event more accurately with fewer curvelet coefficients, which is more pronounced for the noisy data.

Figure 7 is the comparisons of time-frequency analysis obtained by continuous wavelet transform (CWT) and the specialized curvelet transform proposed. The CWT can get the expected effect when the SNR is higher than 10 db. With increasing noise, it can hardly reflect the frequency information of the effective signal. In contrast, when the SNR is

-10 db, the time-frequency analysis by the specialized curvelet transform is equivalent to the result obtained by CWT when the SNR is 10 db. This shows that the proposed method can identify the event better even when the SNR is low.

In order to further verify the reliability of the method, we designed a more intuitive, explicit and targeted model, as shown in Fig. 8(a), which is obtained by convolving the Ricker wavelet with dominant frequency 20 Hz with reflection coefficients with values of 1, -1, 1, 0.7, -0.8 and 0.9 at time 0.340, 0.622, 0.664, 0.964, 1.324 and 1.652 s. Note that the second and third layers form a very small interval. Figure 8(b) is a model with random noise on Fig. 8(a) with SNR of -14.26 db. Figure 8(c,d) is the same trace as in Fig. 8(a,b).

Figure 9(a) shows the results of the proposed specialized curvelet transform for this trace. In comparison to the conventional wavelet transform as shown in Fig. 9(c), the specialized curvelet transform can distinguish the two

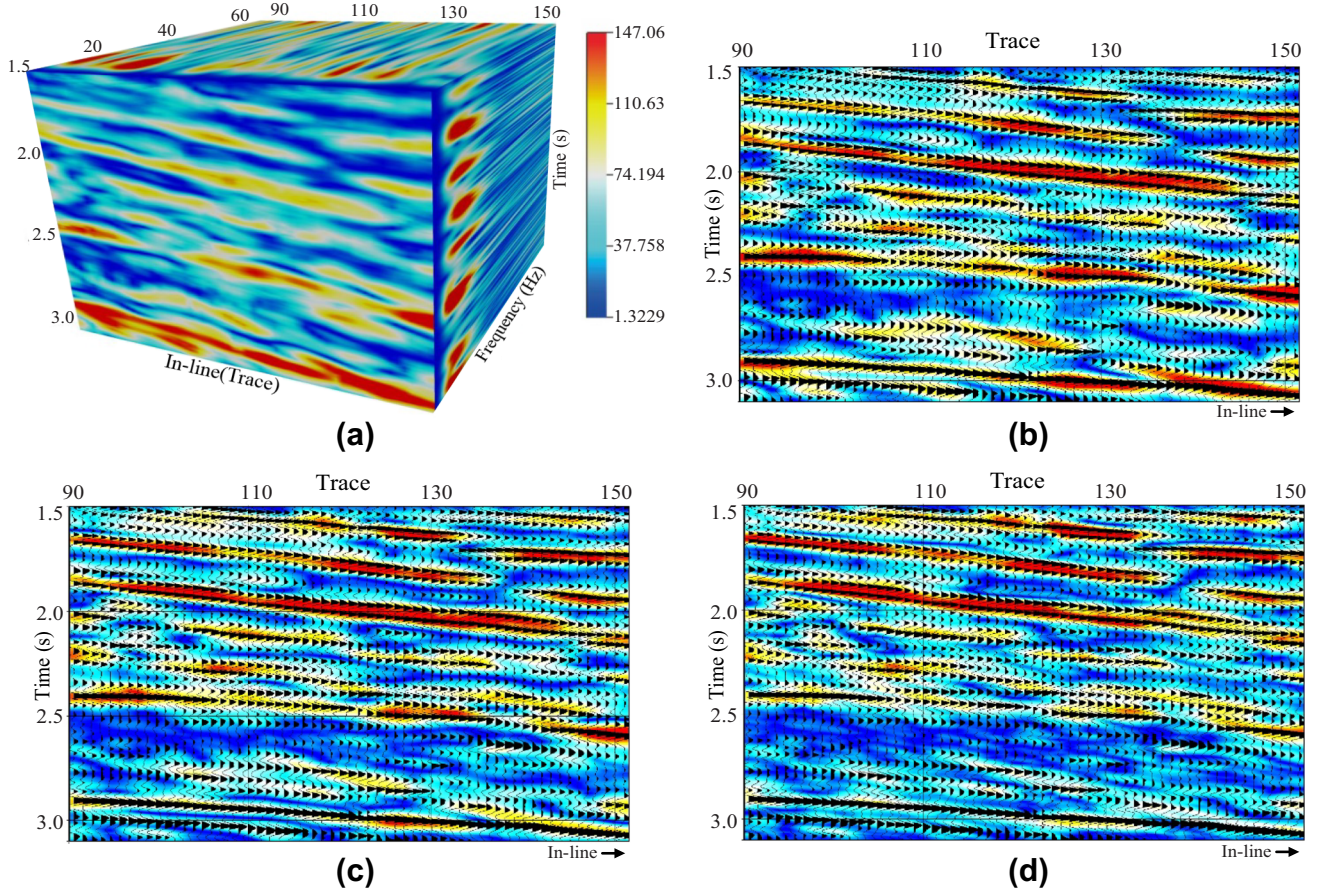


Figure 12 Specialized curvelet transform of multi-trace profile. (a) 3D x - f - t data volume. (b) 16 Hz frequency slice. (c) 20 Hz frequency slice. (d) 26 Hz frequency slice.

adjacent thin layers, which demonstrates the time resolution even in the presence of noise. However, the specialized curvelet transform has a poor frequency resolution. In order to solve this problem, we apply the synchrosqueezing transform in the curvelet transform.

Synchrosqueezing transform is a kind of spectral reassignment method proposed by Daubechies, Lu and Wu (2011), which can make non-stationary and non-linear signals highly focused in time-frequency domain. The basic idea is to map time-scale plane to time-frequency plane using instantaneous frequency estimation $f(a, t)$ for seismic data at offset x_i computed by

$$f_{x_i}(a, t) = -i \text{OASCT}_{x_i}(a, t)^{-1} \frac{\partial \text{OASCT}_{x_i}(a, t)}{2\pi \partial t}, \quad (16)$$

where i is the complex unity. The synchrosqueezing transform $F_{x_i}(f, t)$ is determined only at the centre f_l of the successive bins $[f_l - \frac{1}{2}\Delta f, f_l + \frac{1}{2}\Delta f]$, with $f_l - f_{l-1} = \Delta f$, by the following partial sum over scale values a_k , with

$$a_k - a_{k-1} = (\Delta a)_k,$$

$$F_{x_i}(f_l, t)$$

$$= (\Delta f)^{-1} \sum_{a_k: |f_{x_i}(a_k, t) - f_l| \leq \Delta f/2} \text{OASCT}_{x_i}(a_k, t) a_k^{-\frac{3}{2}} (\Delta a)_k. \quad (17)$$

Figure 9(b) shows the synchrosqueezing transform applied to the specialized curvelet transform. It is clear that after synchrosqueezing processing, the frequency resolution is improved. The dominant frequency is around 20 Hz, and the energy is concentrated in particular events. Even the fourth and fifth events, whose amplitude is relatively weak, are also recognizable in time-frequency domain. Compared with the specialized curvelet transform result shown in Fig. 9(a), synchrosqueezing transform highlights some weaker energy events more clearly, due to the focus on energy. In some cases, the application of the synchrosqueezing transform has great advantages to enhance the time-frequency resolution. But in

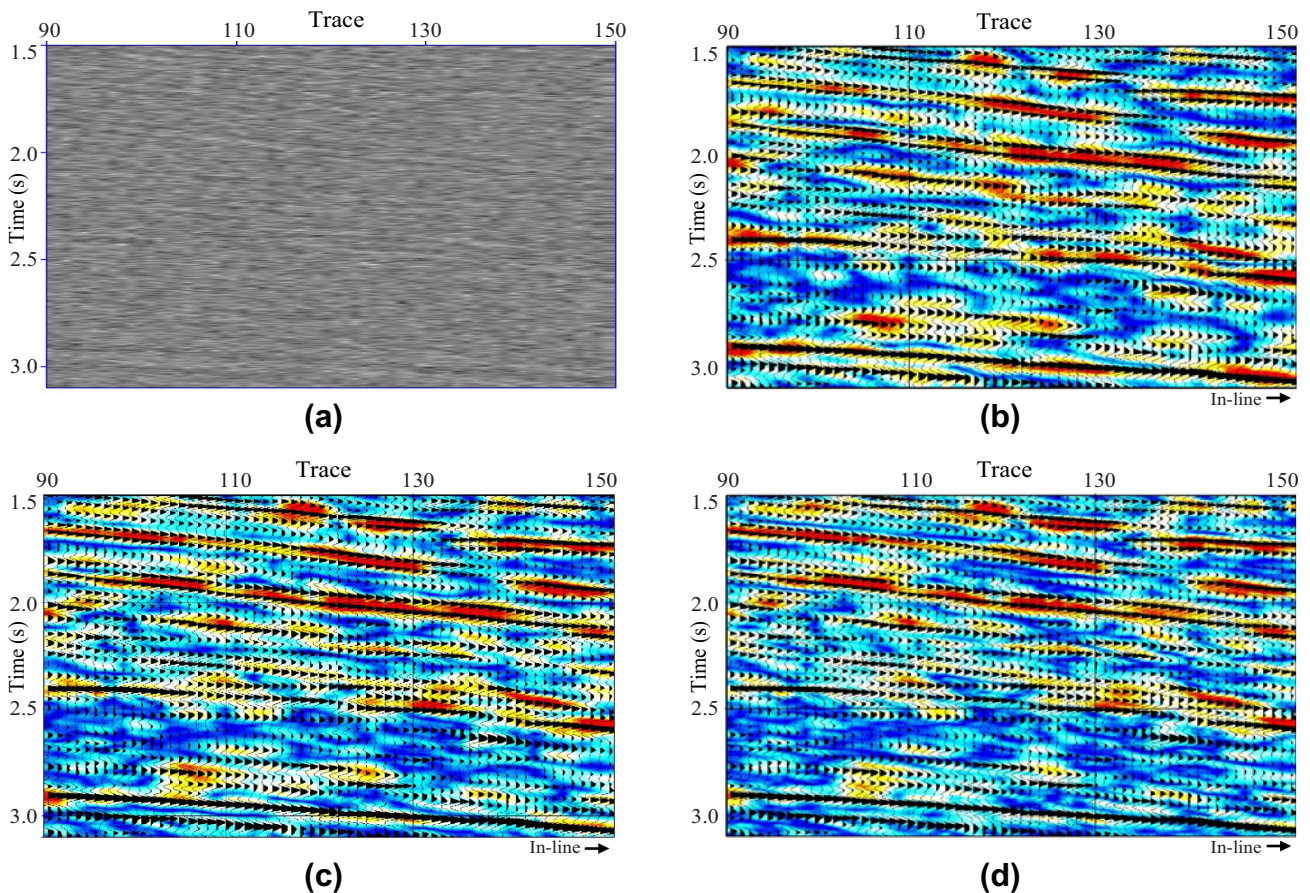


Figure 13 (a) Profile with noise ($\text{SNR} = -14.34 \text{ db}$). Result of the specialized curvelet transform: (b) 16 Hz frequency slice. (c) 20 Hz frequency slice. (d) 26 Hz frequency slice.

some practical applications, a synchrosqueezing transform is not required and we can make a selection based on the data. For comparison, we perform a conventional wavelet transform and synchrosqueezing wavelet transform on the same signal. As shown in Fig. 9(c,d), when SNR is low, the time-frequency analysis result based on wavelet transform is interfered by large amount of noise, and the effective information cannot be identified accurately.

Field data experiment

A single trace processing

The results of the synthetic model test show that the specialized curvelet transform can identify a weak signal among the noise effectively. Now we will show the performance of proposed method for a field data. Figure 10(a) is part of a seismic post-stack profile of field data. Figure 10(b) is the profile with noise, whose SNR is -14.34 db . The events are almost lost

among the noise. Using the same conventions as Fig. 9, we use the specialized curvelet transform, synchrosqueezing specialized curvelet transform, conventional wavelet transform and synchrosqueezing wavelet transform on the 120th trace of record in Fig. 10(b) to get time-frequency plane shown in Fig. 10(c-f), respectively. As indicated by the dotted yellow lines, the method of this paper can more accurately identify the events, and their time location, with a high resolution. In the areas without events, the energy is very weak. As shown in Fig. 10(d), there is a trend shifting energy peaks towards lower frequencies with increasing depth, which satisfies the characteristics of high frequency absorption attenuation in seismic energy with depth. For the wavelet transform, the energy is relatively chaotic and scattered, which can be seen in Fig. 10(e). The energy of the noise completely suppresses the energy of relevant signal information and thus the corresponding events cannot be identified. Because of the multi-scale and multi-azimuthal characteristics of the curvelet transform, and with

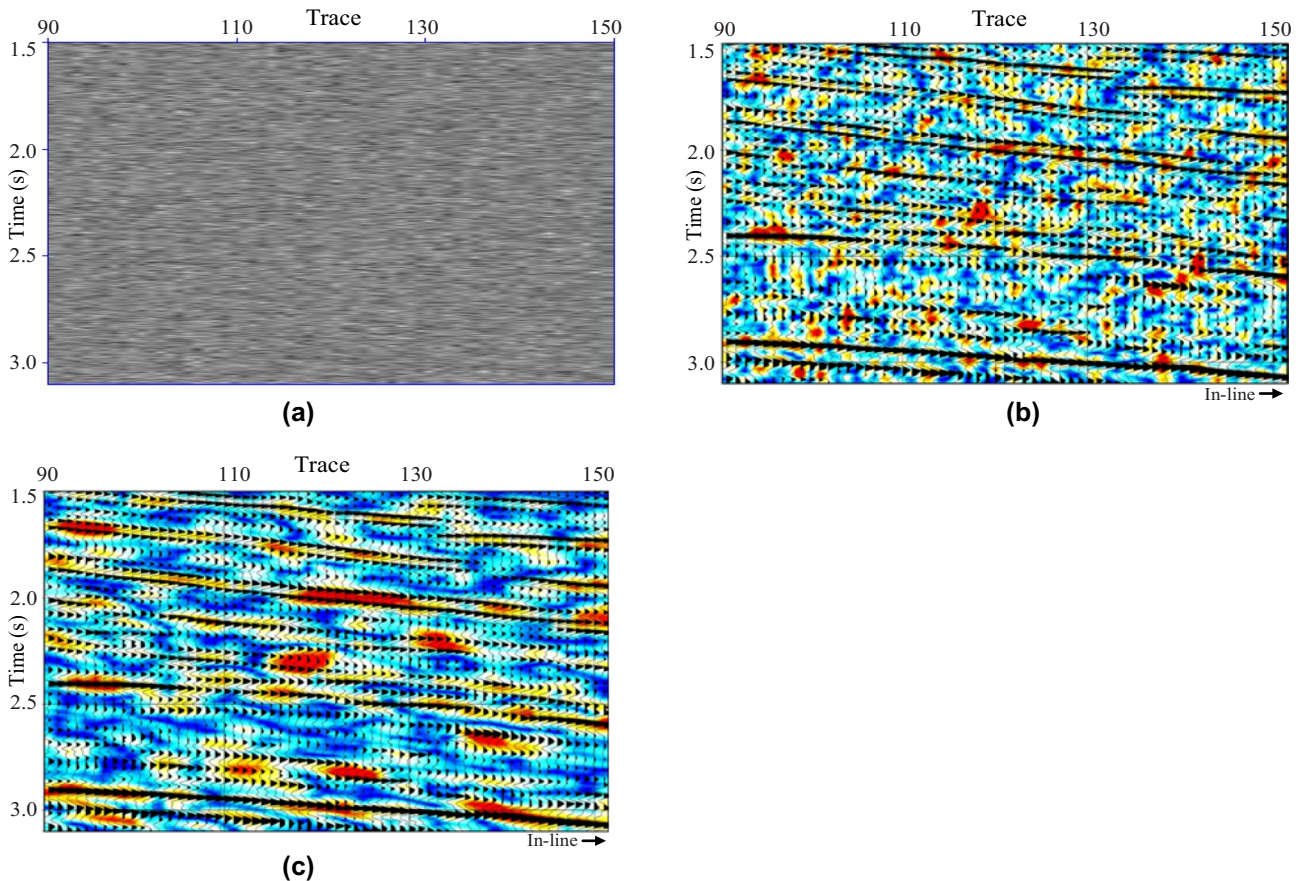


Figure 14 (a) Profile with noise ($\text{SNR} = -18.04 \text{ db}$). (b) 16 Hz frequency slice of wavelet transform. (c) 16 Hz frequency slice of specialized curvelet transform.

the help of improved rotation mode, the specialized curvelet transform has the advantage of identifying the weak signal even within strong noise. The model test and field data processing can both verify the feasibility and effectiveness of the modified method.

Multi-trace processing

In the processing presented above, we only processed a single trace to get the time-frequency plane. We will process all the traces of the profile to get a three-dimensional (3D) (trace-frequency-time) data volume, and display the frequency-trace slice. In order to observe results more conveniently, we take local profile of time window 1.50–3.10 s and trace segments 90–150 (shown in Fig. 11a) for processing and display. Figure 11(b) is the amplitude spectrum of the profile, whose frequency band width is about 10–30 Hz and the dominant frequency is around 20 Hz. Figure 11(c) is the profile with SNR of -4.05 db . Figure 12(a) shows the 3D (trace-

frequency-time) data volume obtained by the specialized curvelet transform on the profile with noise (Fig. 11c). Extracting the frequency slices of 16, 20 and 26 Hz, we get Fig. 12(b–d), respectively. The black waveform is original profile waveform without noise that has been superimposed on the images. The time-frequency energy position is consistent with the position of events, and the energy magnitude corresponds to the amplitude of the events. Due to the attenuation characteristics of the seismic data, the frequency in shallow is higher than that in deep, see Fig. 12(b,d). So the time-frequency energy of the 16 Hz frequency slice is better fit with the deep waveform, while the time-frequency energy of the 26 Hz frequency slice is better fit with the shallow waveform.

Figure 13(a) shows the profile with a lower SNR of -14.34 db , and then we perform specialized curvelet transform on it. With stronger noise, the original information is almost lost in the noise, but after processing, the time-frequency energy can still be relatively concentrated in the strong amplitude events, and the continuity of energy trend and events change

are still identifiable (Fig. 13b–d). When the noise is further increased to SNR –18.04 db, as shown in Fig. 14(a), we cannot identify the original profile information. The low-frequency of wavelet transform is very scattered with no discernible pattern at all (Fig. 14b). Although we cannot identify the events of the original profile, the focus of time-frequency energy is stronger in the specialized curvelet transform, where the correlation with corresponding amplitude of the original event is still strong (Fig. 14c). The outcome of the special curvelet transform is still providing guidance towards the recognition of a weak signal within strong noise.

CONCLUSION

In this paper, we propose a time-frequency domain analysis method based on curvelet transform with time skewing, which is different from the previous idea of random noise attenuation by curvelet transform. We start with the definition of curvelet, adjust the expression of the curvelet transform to make the scale directly related to the frequency of seismic data, so that the curvelet coefficients at different scales can reflect the time-frequency information of seismic data, thereby converting the curvelet coefficients into time-frequency domain. The curvelet coefficients after angle optimized can locate the position of the effective events accurately with fewer curvelet coefficients for the dipping layers, which is more pronounced for the noisy data. Compared with the time-frequency analysis method based on the wavelet transform, the proposed method has an improved ability to identify underlying information for noisy data, and provides a new way for weak signal identification with low signal-to-noise ratio. Numerical tests on synthetic and field data demonstrate the performance of our proposed method.

ACKNOWLEDGEMENTS

This work was supported by the National Science and Technology Major Project (No. 2016ZX05006-002, 2016ZX05024-003-011), the National Key R&D Program of China (No. 2016YFC060110501) and the National Natural Science Foundation of China (No. 41604103). We would like to thank the anonymous reviewers for their helpful comments and suggestions.

REFERENCES

Boustani B., Torabi S., Javaherian A. and Mortazavi S.A. 2013. Ground roll attenuation using a curvelet-SVD filter: a case study

- from the west of Iran. *Journal of Geophysics and Engineering* 10, 055006.
- Candès E. 1998. *Ridgelets: theory and applications*. PhD thesis, Stanford University, Stanford, CA.
- Candès E. and Donoho D. 1999. Curvelets. Technical Report Stanford University, Stanford, CA.
- Candès E. and Donoho D. 2004. New tight frames of curvelets and optimal representations of objects with C2 singularities. *Communications on Pure and Applied Mathematics* 57, 219–266.
- Chauris H. and Nguyen T. 2008. Seismic demigration/migration in the curvelet domain. *Geophysics* 73, S35–S46.
- Daubechies I., Lu J. and Wu H.T. 2011. Synchrosqueezed wavelet transforms: an empirical mode decomposition-like tool. *Applied and Computational Harmonic Analysis* 30, 243–261.
- Dong L., Wang D., Zhang Y. and Zhou D. 2017. Signal enhancement based on complex curvelet transform and complementary ensemble empirical mode decomposition. *Journal of Applied Geophysics* 144, 144–150.
- Donno D., Chauris H. and Noble M. 2010. Curvelet-based multiple prediction. *Geophysics* 75, WB255–WB263.
- Douma H. and de Hoop M.V. 2004. Wave-character preserving pre-stack map migration using curvelets. 74th SEG meeting, Denver, USA, Expanded Abstracts, 961–964.
- Górszczyk A., Malinowski M. and Bellefleur G. 2015. Enhancing 3D post-stack seismic data acquired in hardrock environment using 2D curvelet transform. *Geophysical Prospecting* 63, 903–918.
- Hennenfent G. and Herrmann F. 2004. Three-term amplitude-versus-offset (avo) inversion revisited by curvelet and wavelet transforms. 74th SEG meeting, Denver, USA, Expanded Abstracts, 211–214.
- Herrmann, F.J., Böniger, U. and Verschuur, D.J. 2007. Non-linear primary-multiple separation with directional curvelet frames. *Geophysical Journal International* 170, 781–799.
- Herrmann F.J. and Hennenfent G. 2008. Non-parametric seismic data recovery with curvelet frames. *Geophysical Journal International* 173, 233–248.
- Kumar V. and Herrmann F.J. 2008. Deconvolution with curvelet-domain sparsity. 78th SEG meeting, Las Vegas, USA, Expanded Abstracts, 1996–2000.
- Kustowski B., Cole J., Martin H and Hennenfent, G. 2013. Curvelet noise attenuation with adaptive adjustment for spatio-temporally varying noise. 83th SEG meeting, Houston, USA, Expanded Abstracts, 4299–4303.
- Mallat S.G. 1989. A theory for multiresolution signal decomposition: the wavelet representation. *IEEE Transactions on Pattern Analysis & Machine Intelligence* 11, 674–693.
- Mansinha L., Stockwell R.G. and Lowe R.P. 1997. Pattern analysis with two-dimensional spectral localisation: applications of two-dimensional S transforms. *Physica A: Statistical Mechanics and its Applications* 239, 286–295.
- Naghizadeh M. and Sacchi M.D. 2010. Beyond alias hierarchical scale curvelet interpolation of regularly and irregularly sampled seismic data. *Geophysics* 75, WB189–WB202.

- Neelamani R., Baumstein A.I., Gillard D.G., Hadidi M.T. and Soroka W.L. 2008. Coherent and random noise attenuation using the curvelet transform. *The Leading Edge* 27, 240–248.
- Shahidi R., Tang G., Ma J. and Herrmann, F.J. 2013. Application of randomized sampling schemes to curvelet-based sparsity-promoting seismic data recovery. *Geophysical Prospecting* 61, 973–997.
- Sinha S., Routh P.S., Anno P.D. and Castagna, J.P. 2005. Spectral decomposition of seismic data with continuous-wavelet transform. *Geophysics* 70, 19–25.
- Yarham C., Boeniger U. and Herrmann F. 2006. Curvelet-based ground roll removal. 76th SEG meeting, New Orleans, USA, Expanded Abstracts, 2777–2780.